

ORIGINAL RESEARCH



Potassium alleviates over-reduction of the photosynthetic electron transport chain and helps to maintain photosynthetic function under salt-stress

Yanhui Che¹ | Dayong Fan² | Zhiyuan Teng¹ | Tongtong Yao¹ |
 Zihan Wang¹ | Hongbo Zhang¹ | Guangyu Sun¹ | Huihui Zhang¹ |
 Wah Soon Chow³

¹College of Life Sciences, Northeast Forestry University, Harbin, China

²College of Forestry, Beijing Forestry University, Beijing, China

³Division of Plant Sciences, Research School of Biology, Australian National University, Canberra, Australia

Correspondence

Huihui Zhang, College of Life Sciences, Northeast Forestry University, Harbin 150040, China.

Email: zhang_hh@nefu.edu.cn

Wah Soon Chow, Division of Plant Sciences, Research School of Biology, Australian National University, Canberra, ACT 2601, Australia.

Email: fred.chow@anu.edu.au

Funding information

Fundamental Research Funds for the Central Universities in China, Grant/Award Numbers: 2572018AA24, 2572019DA01; National Key Research and Development Program of China, Grant/Award Number: 2016YFA0600802; National Natural Science Foundation of China, Grant/Award Numbers: 31870373, 31870430; The Third Xinjiang Scientific Expedition Program of China, Grant/Award Number: 2021xjkk0601

Edited by A. Krieger-Liszkay

Abstract

Potassium ions enhance photosynthetic tolerance to salt stress. We hypothesized that potassium ions, by minimizing the trans-thylakoid proton diffusion potential difference, can alleviate over-reduction of the photosynthetic electron transport chain and maintain the functionality of the photosynthetic apparatus. This study investigated the effects of exogenous potassium on the transcription level and activity of proteins related to the photosynthetic electron-transport chain of tobacco seedlings under salt stress. Salt stress retarded the growth of seedlings and caused an outflow of potassium ions from the chloroplast. It also lowered qP (indicator of the oxidation state of Q_A , the primary quinone electron acceptor in Photosystem II (PSII) and Y_{PSII} (average photochemical yield of PSII in the light-adapted state) while increasing Y_{NO+NF} (nonregulatory energy dissipation in functional and nonfunctional PSII), accompanied by decreased expression of most light-harvesting, energy-transduction, and electron-transport genes. However, exogenous potassium prevented these effects due to NaCl. Interestingly, lincomycin (an inhibitor of the synthesis of chloroplast-encoded proteins in PSII) significantly diminished the alleviation effect of exogenous potassium on salt stress. We attribute the comprehensive NaCl-induced downregulation of transcription and photosynthetic activities to retrograde signaling induced by reactive oxygen species. There probably exist at least two types of retrograde signaling induced by reactive oxygen species, distinguished by their sensitivity to lincomycin. Exogenous potassium appears to exert its primary effect by ameliorating the trans-thylakoid proton diffusion potential difference via a potassium channel, thereby accelerating ATP synthesis and carbon assimilation, alleviating over-reduction of the photosynthetic electron transport chain, and maintaining the functionality of photosynthetic proteins.

Yanhui Che and Dayong Fan contributed equally to this study.

This is an open access article under the terms of the [Creative Commons Attribution](https://creativecommons.org/licenses/by/4.0/) License, which permits use, distribution and reproduction in any medium, provided the original work is properly cited.

© 2023 The Authors. *Physiologia Plantarum* published by John Wiley & Sons Ltd on behalf of Scandinavian Plant Physiology Society.

1 | INTRODUCTION

Salt-induced osmotic and ionic stress alters water potential and ionic homeostasis, mainly by inhibiting the efficiency of potassium (K^+) uptake by plants (Arif et al., 2020). Additionally, salt stress negatively impacts key physiological attributes of plants, such as photosynthesis, stomatal activity, leaf chlorophyll content, and seed germination rate (Abdul Qados, 2011; Bistgani et al., 2019; Rahnesan et al., 2018). Furthermore, excessive accumulation of sodium ions impedes the uptake of soil water and nutrients into plants, causing osmotic or water deficit stress and ultimately inhibiting plant growth (Hanin et al., 2016). Regarding the ion homeostasis in cells, when the concentration of Na^+ ions in the cytoplasm is too high, K^+ is displaced by Na^+ , leading to the outflow of potassium ions from the chloroplast (Che, Fan, et al., 2022), which leads to chlorophyll degradation and disruption of the function of photosynthetic proteins (Suo et al., 2017). The accumulation of Na^+ and Cl^- ions has negative impacts on the ultrastructure of the chloroplast photosystem II (PSII), gas exchange, and the transpiration rate, leading to the obstruction of photosynthesis (Khan et al., 2014). Salt stress also prevents the transfer of PSII electrons from the primary quinone receptor Q_A to the secondary quinone receptor Q_B , increasing the probability of charge recombination and generating high levels of singlet O_2 (a ROS species) (Acosta-Motos et al., 2017). When the formation of reactive oxygen species (ROS) exceeds the antioxidant capacity of plants, changes can occur in the activity of various ion channels involved in plant ion homeostasis (Demidchik, 2018), while the PSII reaction center and other photosynthetic proteins are also damaged (Zhang, Wang, et al., 2020). It has been suggested that salt stress aggravates the level of excess absorbed light energy, accumulates high levels of ROS (Miller et al., 2010; Yamane et al., 2012; Zhao et al., 2020), and impairs the PSII repair process (Takahashi & Murata, 2008).

In the process of plant evolution, plants have evolved various strategies by which to adapt to salt stress: (1) increase in the water absorption capacity of plants by increasing osmotic regulatory substances such as soluble sugar and proline (Wang, Ma, et al., 2021); (2) removal of excessive ROS by activating the antioxidative enzyme system to reduce oxidative damage in cells (Zhang, Li, et al., 2020); and (3) combining exogenous salt stress signals with endogenous developmental cues (such as plant hormone signals) *in vivo*, to optimize the balance between growth and stress response (Yu et al., 2020). The photosynthetic system of plants also forms three lines of defense against excess light energy: (1) attenuation of interception and absorption of light energy; (2) protection of the photosystems by avoiding oxidative damage caused by ROS and promoting the dissipation of excess light energy; and (3) repair of PSII injury (PSII turnover) (Dong et al., 2016). Therefore, plant salt tolerance is a complex quantitative trait controlled by multiple genes, which involves salt sensing, signal transduction, osmoregulation, ion transport, hormone synthesis, photosynthesis and metabolism (Yu et al., 2020).

The addition of exogenous potassium ions has been demonstrated to alleviate the damage caused by salt stress to the photosynthetic apparatus, improve the chlorophyll content of leaves under salt

stress and improve the photosynthetic function of leaves (Song et al., 2011). Potassium can also improve osmotic and water potential, reduce stomatal resistance, and increase the number of chloroplast grana, activities of electron transfer and photophosphorylation, activities and contents of ribulose 1,5-bisphosphate carboxylase/oxygenase (Rubisco) and Rubisco activase, and net photosynthetic rate (Zheng et al., 2002). Overexpression of thylakoid K^+/H^+ antiporter KEA_3 accelerates relaxation of photoprotective energy-dependent quenching after transitioning from high-light to low-light conditions in *Arabidopsis thaliana* and tobacco (Armbruster et al., 2016). Other studies have shown that retention of K^+ , inhibition of excessive accumulation of Na^+ , and maintenance of a high K^+/Na^+ ratio mediated by an H^+/K^+ antiporter induce tolerance traits in salt-sensitive plants (Wang et al., 2017). Triple mutations of K^+ outflow antiporters, such as $AtKEA1$, $AtKEA2$, and $AtKEA3$, substantially changed chloroplast development and proton dynamics on the thylakoid membrane, leading to diminution of carbon assimilation and growth rate (Kunz et al., 2014). Thus, potassium ions play important roles in pigment restoration, energy quenching, carbon assimilation and ion balance, among other functions.

The large amount of ROS produced under salt stress may lead to retrograde signal transduction (Crawford et al., 2018), downregulating the transcription level of most genes related to energy harvesting, conversion, and utilization of the electron transport chain. However, there have been relatively few studies on the involvement of potassium ions in alleviating retrograde signaling (Che, Yao, et al., 2022; Wu et al., 2018) and damage to PSII (Ball et al., 1987; Bezerra et al., 2021; Che, Fan, et al., 2022; Chow et al., 1990) under salt stress. Furthermore, alleviation by K^+ is often dependent on the concentration present in the growth medium (Bezerra et al., 2021; Chow et al., 1990); a higher K^+ concentration allows greater retention of cytosolic K^+ , which allows a plant to accumulate high amounts of Na^+ in the cytosol without compromising the cytosolic K^+/Na^+ ratio. This ratio determines cell metabolic competence and, therefore, the ability of a plant to survive in a salt-stress environment (Zhao et al., 2020).

In our previous study with mulberry (Che, Fan, et al., 2022), the results were consistent with an enhanced proton diffusion potential difference that developed across the thylakoid membrane during salt stress. Additionally, in our previous study with tobacco (Che, Yao, et al., 2022), the H_2O_2 content was increased, accompanied by altered activities of anti-oxidative enzymes, during salt stress. Combining these results or their interpretation, in this study with tobacco we aimed to further test the hypothesis that (1) salt stress leads to over-reduction of the electron transport chain, a phenomenon in which, due to the depletion of stromal K^+ under salt stress, K^+ ions are unable to enter the thylakoid lumen rapidly enough to charge-compensate for the efflux of H^+ from the lumen via the ATP synthase, resulting in insufficient ATP to support rapid carbon assimilation; (2) a consequent over-reduced electron transport chain enhances the formation of H_2O_2 and singlet oxygen, both of which could lead to retrograde signaling (Chan et al., 2016; Foyer & Shigeoka, 2011; Gollan et al., 2015) that affects the expression of many genes involved in photosynthesis; and (3) supplemental potassium can prevent many of

the effects of salt stress primarily by alleviating the trans-thylakoid proton diffusion potential difference via rapid charge compensation through a potassium channel as protons exit the thylakoid lumen via the ATP synthase.

2 | MATERIALS AND METHODS

2.1 | Plant material and growth conditions

The present experiments were conducted at the Laboratory of Plant Physiology, Northeast Forestry University, Harbin, China. Tobacco seeds were sown into holes in a 5 × 10 cm plate. When tobacco seedlings had grown to 5 cm, they were transplanted into 13-cm diameter, 15-cm tall pots filled with a 2:1 (v/v) mixture of peat soil and vermiculite. Seedlings were maintained at 25/23°C (light at 400 μmol photons m⁻² s⁻¹, photoperiod 12/12 h light/dark) and relative humidity of about 65%. The plants were watered with ½ strength Hoagland nutrient solution once a week. When each plant had grown five true leaves, the following different treatments were applied: (1) H₂O; (2) 150 mM NaCl; (3) 150 mM NaCl + 20 mM KCl; and (4) 150 mM NaCl + 20 mM KCl + 1 mM lincomycin (Linco). Each pot was individually watered with the selected solution; each pot had a saucer at the bottom to catch any solution seeping through the pot when the solution was supplied to the top of the pot. When the soil became dry, the solution in the saucer would be re-absorbed into the soil. In the salinity treatments (3) and (4), the ratio of K⁺ to Na⁺ (0.13) was approximately comparable to that in other studies of salinity stress: 0.02 in Ball et al. (1987), 0.04 in Chow et al. (1990), 0.05–0.10 in Ahanger and Agarwal (2017), 0.02–0.06 in Bezerra et al. (2021) and 0.02 in Che, Fan, et al. (2022). The control (H₂O treatment) utilized added distilled water only. For all plants, 200 mL of solution was poured into the dish each time, and 200 mL of solution was added each time the dish was dry. After 5 days of treatment, plant indexes were determined and recorded.

2.2 | Seed germination

Twenty-five seeds were placed on two pieces of qualitative filter paper in a Petri dish, after which 3 mL of the various treatment solutions were added to each dish with an eye dropper to soak all the filter paper to ensure the seeds would absorb the solution. When the germinated seeds had each grown two leaves, images were captured, and root length was measured.

2.3 | Isolation of chloroplasts and determination of potassium ion content

Chloroplasts were isolated from tobacco leaves, as previously described for mulberry leaves (Che, Fan, et al., 2022). K⁺ and Na⁺ contents were determined by atomic absorption spectrophotometry

in both tobacco leaf tissue and isolated chloroplasts after digestion, as described by Che, Fan, et al. (2022). In these measurements, the NaCl + K + Linco treatment was not included.

2.4 | Chlorophyll content

First, 0.1 g of fresh leaf sample was ground to a homogenate in a mortar containing 96% ethanol, and then the sample was allowed to stand for 3–5 min after fading before proceeding. The extract was filtered through a filter paper funnel into a 25-mL brown volumetric flask, topped with 96% ethanol to a constant volume. With 96% ethanol as a blank control, the absorbance was measured at wavelengths 665, 649, and 470 nm. The concentrations of extracted chlorophylls ([C_a] [C_b]) and carotenoids ([Car]) were calculated as: [C_a] = 13.96 OD₆₆₅ – 6.88 OD₆₄₉; [C_b] = 24.96 OD₆₄₉ – 7.32 OD₆₆₅; and [Car] = (1000 OD₄₇₀ – 2.05C_a – 114.8C_b)/245 (Feng et al., 2022; Li, 2000; Liu et al., 2010).

2.5 | Expression levels of related genes

The total RNA was extracted from plant tissue samples smaller than 100 mg using the OMEGA plant RNA Kit (Bio-Tek, USA) kit, and then, single-stranded cDNA template synthesis (Che, Fan, et al., 2022) was conducted with the ReverTra Ace qPCR RT Kit (Toyobo, Japan) and the premixed dye FastStart Universal SYBR Green Master (ROX) (Roche, Switzerland). The amplification was conducted using a Mastercycler[®] nexus series PCR instrument (Eppendorf, Germany). After amplification, semi-quantitative PCR was conducted using agarose gel electrophoresis. The following gene-specific primers (5'–3') were used: *psbA* F, ATGCGACCTTGGATTGCTGTTG; *psbA* R, ACCATGAGCGGCTACGATGTTAT; *atpB* F, GTATTTGGCGGAGTGGGTGAAC; *atpB* R, CACAGCGGAAGGCATTCTACC.

2.6 | Transcriptome analysis

Cut tobacco leaves from the three treatments were wrapped in aluminum foil and frozen in liquid nitrogen for 1 h. All the samples were then sent to Hua da Gene Sequencing Co. Ltd. (China) for transcriptome analysis. RNA-Seq (Quantification) based on next-generation high-throughput sequencing technology was used to study the gene expression pattern and provide accurate digital expression profiles by sequencing and comparing transcripts. In brief, the experimental procedure included the following steps: mRNA isolation, mRNA fragmentation, cDNA synthesis, end repair, addition of poly-A tails and adaptor ligation, PCR, library quality control, circularization, and sequencing.

The sequence data were filtered with SOAPnuke (v1.5.2) (<https://github.com/BGI-flexlab/SOAPnuke>) and the clean reads were mapped to the reference genome using HISAT2 (v2.0.4) (<http://www.ccb.jhu.edu/software/hisat/index.shtml>). The clean reads were aligned with

the reference gene set by Bowtie2 (v2.2.5) (<http://bowtiebio.sourceforge.net/Bowtie2/index.shtml>), and the gene expression level was calculated by RSEM (v1.2.12) (<https://github.com/deweylab/RSEM>). Kyoto Encyclopedia of Genes and Genomes (KEGG) (<https://www.kegg.jp/>) enrichment analysis of expressed genes was conducted using Phyper. The significance levels of the KEGG terms and pathways were corrected using a Q-value with a strict threshold (Q-value ≤ 0.05).

2.7 | Chlorophyll fluorescence kinetics curve

The chlorophyll fluorescence kinetics curve was measured using a Multi-Function Plant Efficiency Analyser (M-PEA) (Hansatech, King's Lynn, UK) after dark adaptation for 30 min. To determine the OJIP curve, a pulse of red light ($3500 \mu\text{mol m}^{-2} \text{s}^{-1}$) was applied, and the chlorophyll fluorescence signal was recorded for 1 s (Wang et al., 2022). The time nodes of relative fluorescence intensity F_0 , F_J , F_I and F_P , at points O, J, I, and P, are 0.02, 2, 30 and 1000 ms, respectively (Che et al., 2020), and the relative fluorescence curve can be described as $V_{O-P} = (V_t - V_0)/(V_P - V_0)$, where the subscript t denotes time t . The difference between the value of each treatment and the H_2O treatment value is ΔV_{O-P} . The relative fluorescence curve of points O–K is $W_{OK} (\text{L-band}) = (V_t - V_0)/(V_K - V_0)$, where K is an inflection point at 0.3 ms, and ΔW_{OK} is obtained from the difference between the treatment and H_2O control. Additionally, O–J curve W_{OJ} (K-band), ΔW_{OJ} , I–P curve W_{IP} (G-band), ΔW_{IP} , W_{OI} , and ΔW_{OI} (Momchil et al., 2018) can be similarly obtained.

2.8 | Chlorophyll fluorescence parameters related to PSII

Leaves were first dark adapted for 30 min. The initial fluorescence (F_0) and maximum fluorescence (F_m) were measured using an FMS-2 pulse modulation fluorimeter (Hansatech, King's Lynn, UK) to calculate the dark-adapted maximum quantum efficiency of PSII photochemistry (F_v/F_m). Then, under illumination for 3 min at an irradiance of $500 \mu\text{mol m}^{-2} \text{s}^{-1}$, the following were measured: (1) the photochemical yield of PSII averaged over closed and open PSII traps (Y_{II}); (2) the fraction of light absorbed by PSII that is nonphotochemically dissipated in a light-regulated manner, (Y_{NPQ}); (3) the sum of the fraction of light absorbed by PSII that is dissipated in a constitutive, unregulated manner and that which is emitted as chlorophyll fluorescence (Y_{NO+NF}) from both functional and nonfunctional PSII; (4) the chlorophyll fluorescence parameters qP (an indicator of the oxidation state of Q_A in the puddle model) and (5) the photochemical efficiency of open PSII traps (F_v'/F_m'). Calculation and determination of the following parameters were conducted according to the method described by Kornyeyev and Hendrickson (2007), who considered the PSII pool as a whole without splitting it into functional and nonfunctional (NF) subpopulations: $Y_{II} = 1 - F_s/F_m'$; $Y_{NPQ} = F_s/F_m' - F_s/F_m$; $Y_{NO+NF} = F_s/F_m$. Here, F_m refers to the dark-adapted

maximum fluorescence yield when there may or may not be photo-inactivated PSII complexes present ($= [F_m]_{PI}$, as used by Kornyeyev & Hendrickson, 2007). $Y_{II} + Y_{NPQ} + Y_{NO+NF} = 1$. The parameters qP and F_v'/F_m' were calculated as described by Che, Fan, et al. (2022).

2.9 | Measurement of the MR820 signal

The MR820 optical reflection signal (MR820) was determined by an M-PEA Multi-Function Plant Efficiency Analyser. The second fully developed leaf of a tobacco seedling was dark-adapted for 0.5 h before measurement. The measurement site was between the third and fourth leaf veins from the leaf base, about 2 cm from the main leaf vein. A downward signal indicates P700 oxidation (less transmission or reflection of the 820 nm measuring beam absorbed by P700^+). Based on the measurement data obtained, we standardized the first point of the pre-illumination signal by setting it as “1.” The difference between the lowest and highest points can qualitatively represent PSI activity, but not quantitatively (Oukarroum et al., 2013). The activity of the PS I reaction center was expressed as the relative difference between the maximum (I_0) and the minimum (I_{\min}) reflectance at 820 nm, namely, $\Delta I/I_0 = (I_0 - I_{\min})/I_0$.

2.10 | Data processing

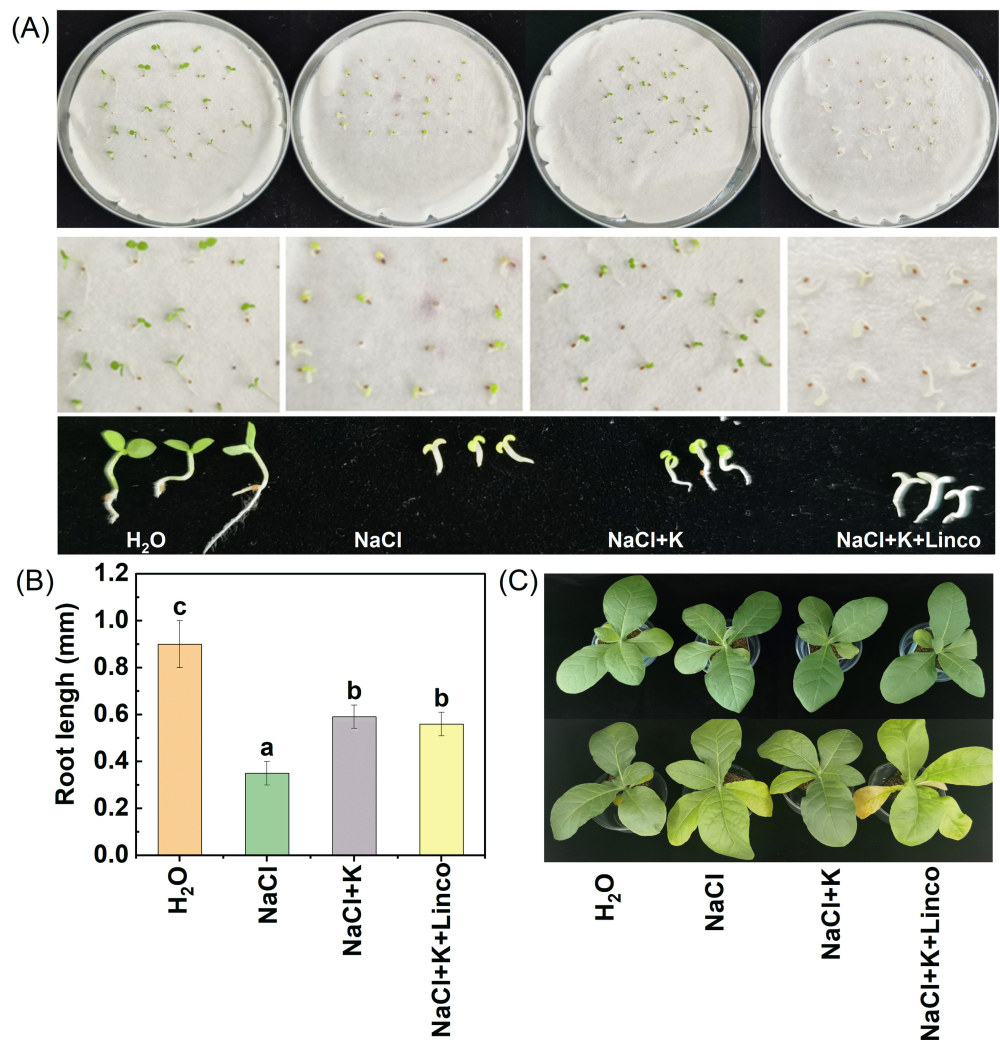
Excel (Office, 2016; Microsoft Corp., USA) and SPSS 22.0 (IBM Corp., USA) were used for statistical analysis. Origin2019bis (OriginLab, USA) was used for drawing the figures. Single factor analysis of variance (ANOVA) and least significant difference (LSD) procedures were used to compare differences among treatment groups. Each parameter was determined in triplicate.

3 | RESULTS

3.1 | Exogenous K^+ alleviates the NaCl-induced inhibition of postgermination plant morphology and development in tobacco

As shown in Figure 1A, although there was no significant difference in the germination rate of tobacco seeds among the four treatments, NaCl affected the vegetative growth of tobacco seedlings. Compared with the control H_2O treatment, NaCl treatment for 5 days significantly decreased the cotyledon area, reduced the root length and induced cotyledon yellowing. Compared with the NaCl treatment, the application of K^+ significantly increased the cotyledon area, increased radicle length (Figure 1B) and induced greener cotyledons (Figure 1A). Root length under the NaCl + K + Linco treatment was also significantly greater than that under NaCl; there was no difference in root length between NaCl + K and NaCl + K + Linco treatments, but the cotyledons of NaCl + K + Linco-treated plants were pale green or white (Figure 1A). This indicates that the inhibition of synthesis of D1

FIGURE 1 Effects of four treatments on (A) germinated seedling morphology, (B) root length, and (C) leaf morphology. (A) Twenty-five seeds were placed in each Petri dish, and the filter papers were changed every 2 days. (B) After the seeds had germinated, root length was measured after seedlings had developed two mature cotyledons. (C) Plants before (above) and after (below) 5 days of treatment.



and other chloroplast-encoded proteins (despite repair of PSII being potentially aided by potassium ions, Chow et al., 1990) can seriously affect the synthesis of chlorophyll.

In addition, NaCl had a significant effect on tobacco seedlings that were already in the vegetative growth phase. As shown in Figure 1C, leaves of tobacco plants treated with NaCl for 5 days showed yellowing, while K⁺ restored the leaf color to the H₂O control level. However, after adding lincomycin, leaf chlorosis was evident in the widespread yellowing (Figure 1C), which means that K⁺ may prevent leaf yellowing by promoting the synthesis of PSII proteins in the absence of lincomycin.

In the NaCl treatment, the potassium ion content in the leaf tissue was much decreased compared with the H₂O treatment (Figure 2A). Importantly, the K⁺ content of chloroplasts was only half of that of the H₂O treatment (Figure 2B). By contrast, the K⁺ content leaf tissue and chloroplasts reached levels of the H₂O treatment when NaCl was supplemented by K⁺ (Figure 2A,B). The Na⁺ content of leaf tissue was greatly increased in both the NaCl treatment and NaCl + K treatment relative to the H₂O treatment (Figure 2C), but supplementing NaCl with K⁺ brought the Na⁺ content of chloroplasts back to approximately the level of the H₂O Treatment (Figure 2D). The ratio

of K⁺ in chloroplasts to that in leaf tissue was decreased in the NaCl treatment relative to the H₂O treatment (Figure 2E). The ratio of Na⁺ in chloroplasts to that in leaf tissue was much decreased in both the NaCl and NaCl + K treatments relative to the H₂O treatment (Figure 2F).

3.2 | Chlorophyll content and expression of related genes

As shown in Figure 3, compared with the H₂O treatment, NaCl significantly decreased the chlorophyll *b* content of tobacco leaves but had no significant effect on the chlorophyll *a* content. In the NaCl + K treatment, the content of chlorophyll *a* and chlorophyll *b* increased compared with the NaCl treatment and reached or exceeded the level of the H₂O treatment. After adding lincomycin, the chlorophyll (*a* + *b*) content was lower than that of the NaCl + K treatment but slightly higher than that of the NaCl treatment. Relative to the H₂O treatment, both NaCl and NaCl + K + Linco treatments decreased the content of chlorophyll *a* + *b*, while the NaCl + K treatment increased the total chlorophyll content (Figure 3C).

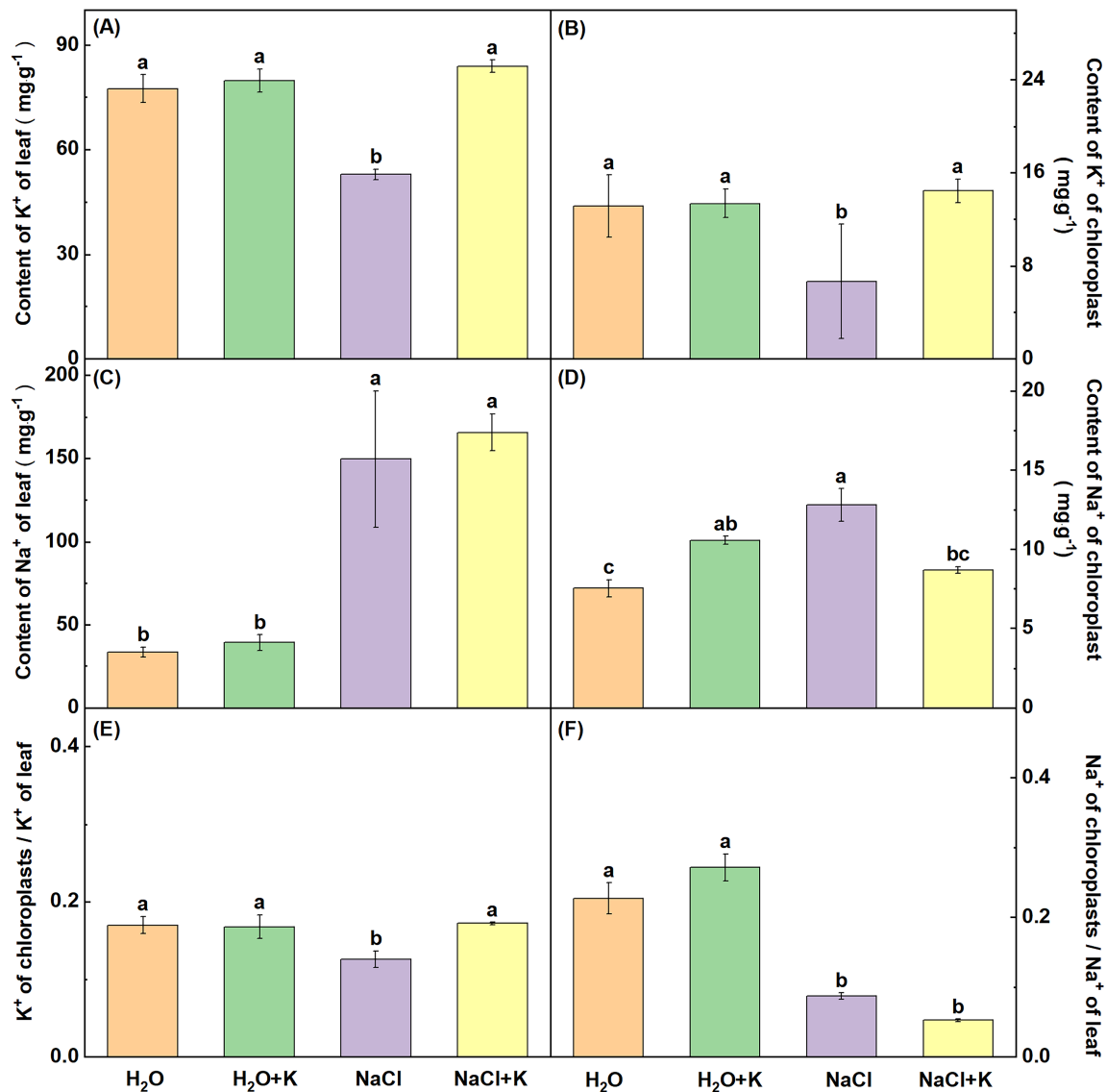


FIGURE 2 Contents of K⁺ and Na⁺ in leaf tissue and chloroplasts in treatments with H₂O, H₂O + K, NaCl and NaCl + K. (A) K⁺ content per g fresh weight of leaf tissue; (B) K⁺ content in chloroplasts per g fresh weight of leaf tissue; (C) Na⁺ content per g fresh weight of leaf tissue; (D) Na⁺ content in chloroplasts per g fresh weight of leaf tissue; (E) Ratio of K⁺ content in chloroplasts to K⁺ content in leaf tissue; (F) Ratio of Na⁺ content in chloroplasts to Na⁺ content in leaf tissue.

Compared with the H₂O treatment, the transcription of 21 chlorophyll synthesis genes (*Glu-TR* [LOC107763283, LOC107781666], *ALAD* [LOC107793287, LOC107798564], *PBGD* [LOC107802823, LOC107802603, LOC107830132, LOC107767993], *UROS* [LOC10778553, LOC107797441], *CPOX* [LOC107766888], *PPOX* [LOC107780878, LOC107827378], *POR* [LOC107787316, LOC107820326, LOC107795891, LOC107793976, LOC107825540, LOC107804928], *DVR* [LOC107806278, LOC107773288]) in the NaCl treatment was significantly downregulated (Figure 3D), and the expression levels of chlorophyll *b* degradation genes (*PPH* [LOC107789349, LOC107787339, LOC107763257, LOC107824158]) were higher than those in the H₂O treatment on the whole (Figure 3E), consistent with the decrease in chlorophyll *b* content. Compared with the NaCl treatment, 20 chlorophyll synthesis genes

were significantly upregulated after the NaCl + K treatment; among these, all *PBGD*-related genes were upregulated, but chlorophyll *b* degradation genes were downregulated overall. After the NaCl + K + Linco treatment, 33 chlorophyll synthesis genes were significantly downregulated, and 7 chlorophyll degradation genes were significantly upregulated compared with the H₂O treatment (see Figure 3 for details).

3.3 | Carotenoid content and related gene expression

As shown in Figure 4A, carotenoid content increased under NaCl and NaCl + K + Linco treatments but not significantly compared with the

H₂O treatment. The NaCl + K treatment, however, significantly increased carotenoid content compared with the H₂O treatment (Figure 4A). Transcriptome data showed that *PDS* (LOC107816873), and *ZE* (LOC107797654, LOC107763949) genes were slightly

upregulated under salt stress compared with the H₂O treatment, while *GGPS* (LOC107767572, LOC107799556), *LBCY* (LOC107830918), *VDE* (LOC107763628, LOC107780507), and *LCYE* (LOC107830918, LOC107789691) were slightly downregulated in NaCl + K

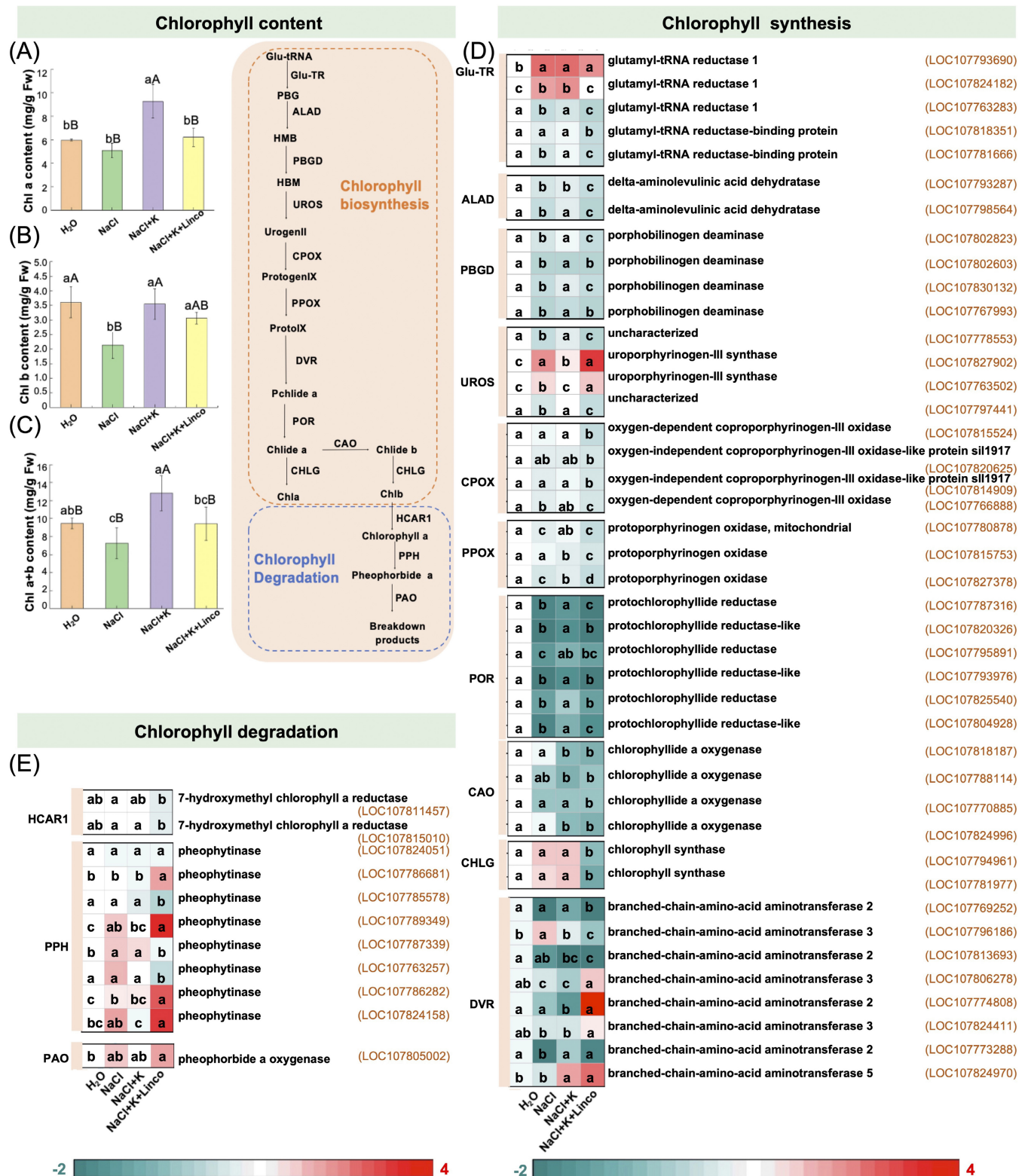


FIGURE 3 Legend on next page.

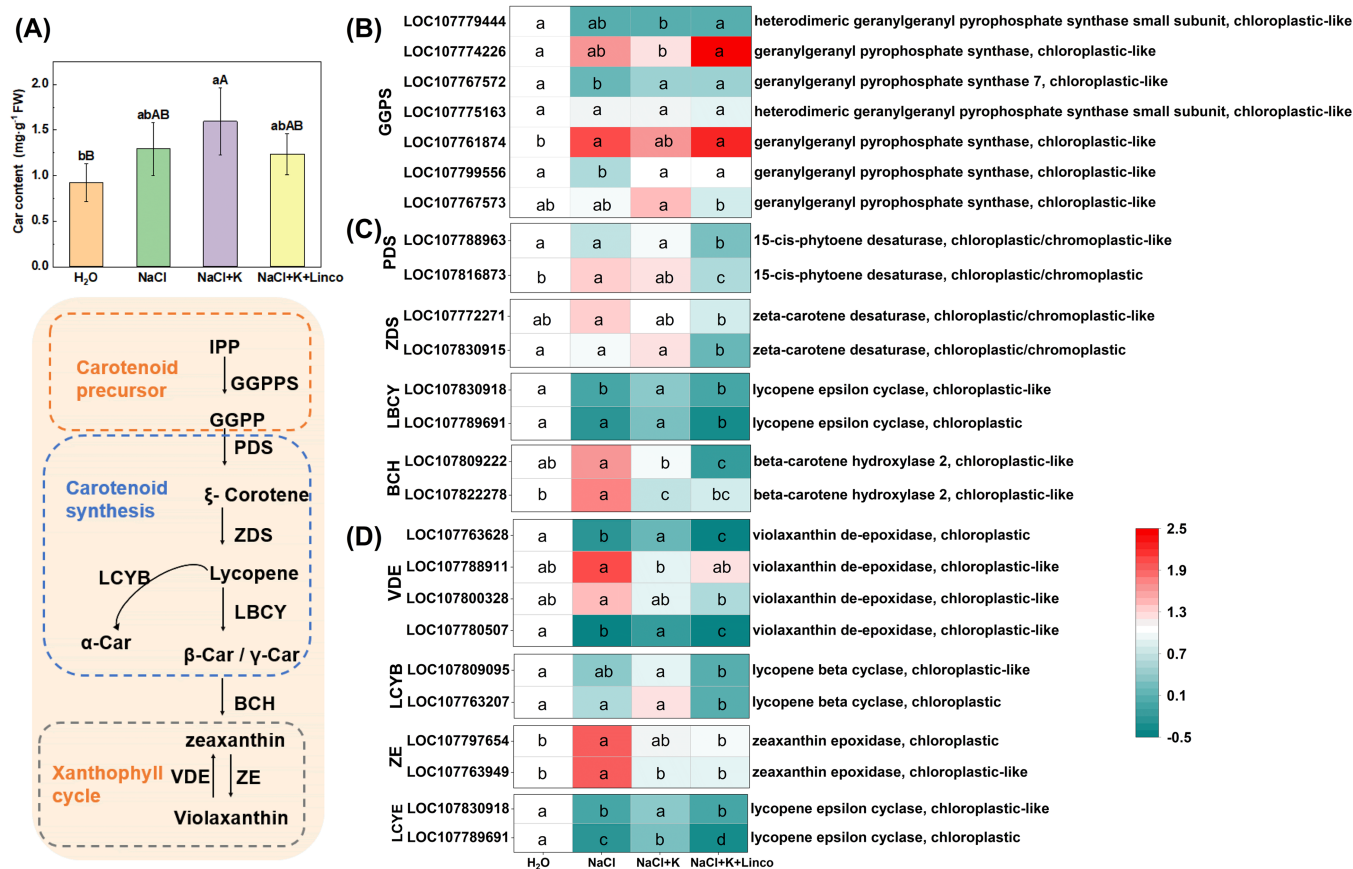


FIGURE 4 Effect of potassium ions on carotenoid content (A) and the expression of related genes under salt stress (B–D). IPP, isopentene pyrophosphate; GGPPS, geranylgeranyl pyrophosphate synthase; GGPP, geranylgeranyl pyrophosphate; PDS, 15-cis-phytoene desaturase; ZDS, zeta-carotene desaturase; LCYB, lycopene beta cyclase; LCYE, lycopene epsilon cyclase; LBCY, lycopene epsilon cyclase; BCH, beta-carotene hydroxylase; VDE, violaxanthin de-epoxidase; ZE, zeaxanthin epoxidase. The values shown in the heat map become progressively larger from blue to red, and the columns of the heat map correspond to the H₂O, NaCl, NaCl + K, and NaCl + K + Linco treatments, respectively from left to right. Significant differences according to least significant difference (LSD) tests are indicated by different lowercase letters ($p < 0.05$).

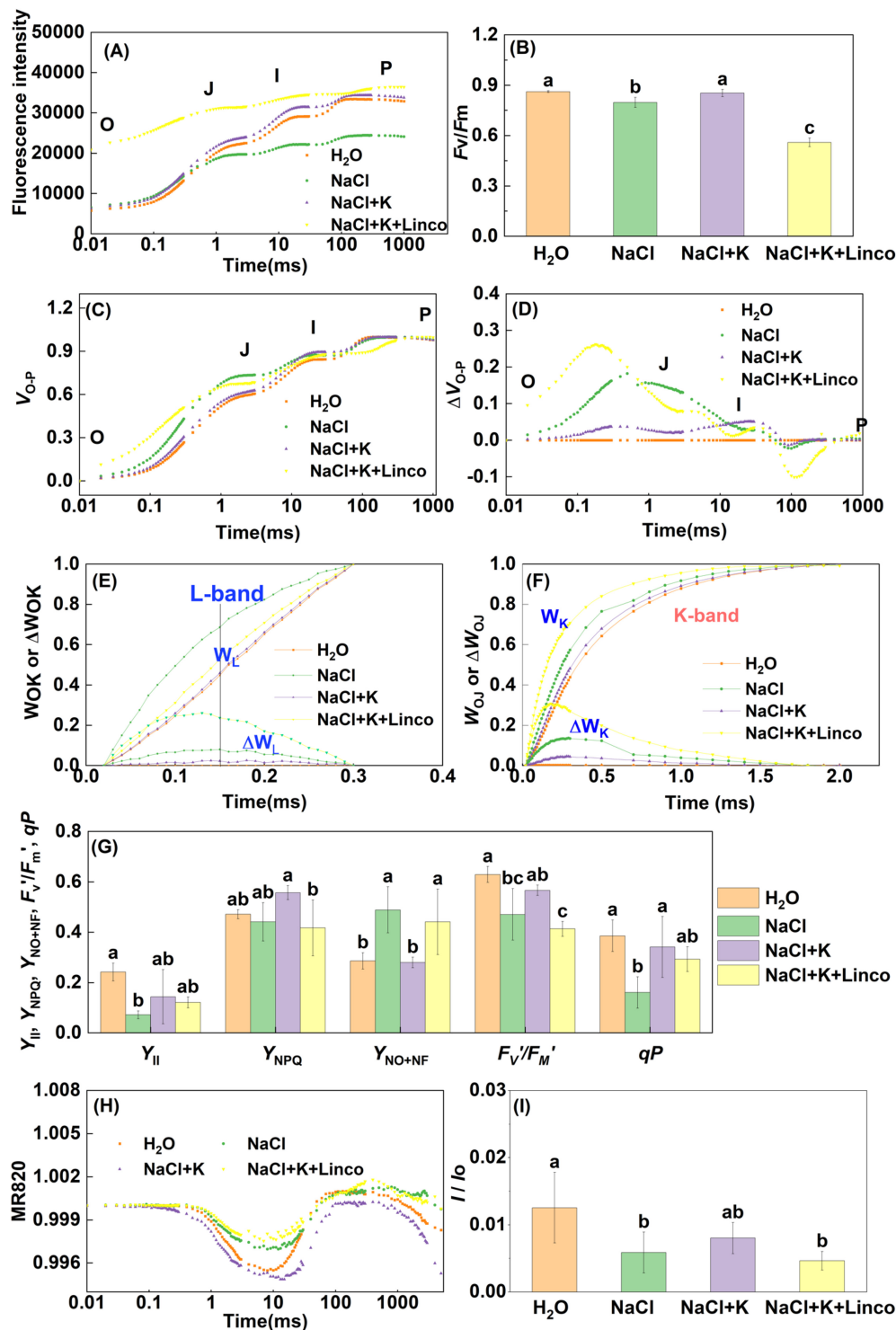
treatment compared with the H₂O treatment. After potassium was added to the salt stress treatment, seven genes were significantly upregulated relative to the NaCl treatment, namely, GGPS (LOC107767572, LOC107799556), LBCY (LOC107830918), VDE (LOC107763628, LOC107780507), LCYE (LOC107830918, LOC107789691), while four genes (LOC107809222, LOC107822278, LOC107788911, LOC107763949) were significantly downregulated compared with the NaCl treatment (Figure 4B–D), indicating that potassium ions play an important role in regulating carotenoid biosynthesis.

3.4 | Fluorescence parameters related to PSII and PSI

The OJIP fluorescence intensity curves show that the latter half of the OJIP curve of the NaCl treatment was lower than that of the H₂O treatment. By contrast, the OJIP curve of the NaCl + K + Linco treatment was higher than that of the H₂O treatment throughout, the increase in F_0 under NaCl + K + Linco being suggestive of inactivation of PSII reaction centers. Additionally, the OJIP curve of the NaCl + K treatment was similar to that of the

FIGURE 3 Effects of potassium ions on contents of chlorophyll (A–C) and its related synthesis (D) and degradation (E) genes in tobacco leaves under salt stress. Glu-TR, glutamyl-tRNA reductase; Glu-tRNA, L-glutamyl-tRNA; PBG, porphobilinogen; ALAD, delta-aminolevulinic acid dehydratase; HMB, hydroxymethylbilane; PBGD, porphobilinogen; deaminase; UROS, uroporphyrinogen III synthase; Urogen II, uroporphyrinogen II; CPOX, coproporphyrinogen-III oxidase; Protogen IX, protoporphyrinogen IX; PPOX, protoporphyrinogen oxidase; DVR, branched-chain-amino-acid aminotransferase; Pchlide a, protochlorophyllide a; POR, light-dependent protochlorophyllide oxidoreductase; Chlide a, chlorophyllide a; CHLG, protoporphyrin IX Mg-chelatase subunit G; Chl a, chlorophyll a; CAO, chlorophyllide a oxygenase; Chlide b, chlorophyllide b; Chl b, Chlorophyll b; HCAR, 7-hydroxymethyl chlorophyll a reductase; PPH, pheophytinase; PAO, pheophorbide a oxygenase. The values shown in the heat map become progressively larger from blue to red, and the columns of the heat map correspond to the H₂O, NaCl, NaCl + K, and NaCl + K + Linco treatments, respectively from left to right. Significant differences according to least significant difference (LSD) tests are indicated by different lower-case letters ($p < 0.05$).

FIGURE 5 Effects of potassium ions on parameters related to photosystem I and II in tobacco leaves under salt stress. (A) fluorescence curve under different treatments; (B) F_v/F_m , maximum fluorescence; (C) fluorescence curve from O point to P point; (D) $\Delta V_{O-P} = V_{O-P}(\text{treatment}) - V_{O-P}(\text{H}_2\text{O})$; (E) W_{OK} is the fluorescence curve of points O-K, W_{OK} (L-band) = $(V_t - V_O)/(V_K - V_O)$, and so on; (G) the fluorescence parameters Y_{II} , Y_{NPQ+NF} , Y_{NO} , F_v/F_m' , and qP ; (H) the light-induced change in absorption at 820 nm can indicate the activity of PSI; and (I) quantification of the difference between the lowest point and the highest point of MR820.



H₂O treatment (Figure 5A). After salt stress treatment, F_v/F_m was slightly reduced compared with the H₂O treatment; after potassium supplementation, F_v/F_m was slightly increased compared with the NaCl treatment; after PSII repair was inhibited by lincomycin, F_v/F_m was as low as 0.55 (Figure 5B). As can be seen from the O-P curve when normalized to the peak value, the J point under salt stress occurred at about 1 ms, while that under the NaCl + K + Linco treatment appeared earlier than that of the NaCl treatment, at

about 0.3 ms. Potassium supplementation under salt stress significantly elevated the J point of these two curves compared with the H₂O treatment (Figure 5C,D).

W_{OK} and W_{OJ} curves showed that the positive L- and K-bands in the NaCl + K + Linco treatment were significantly higher than those in other treatments, followed by those in the NaCl treatment. The L- and K-bands of the NaCl + K treatment are close to the level of the H₂O treatment (Figure 5E,F).

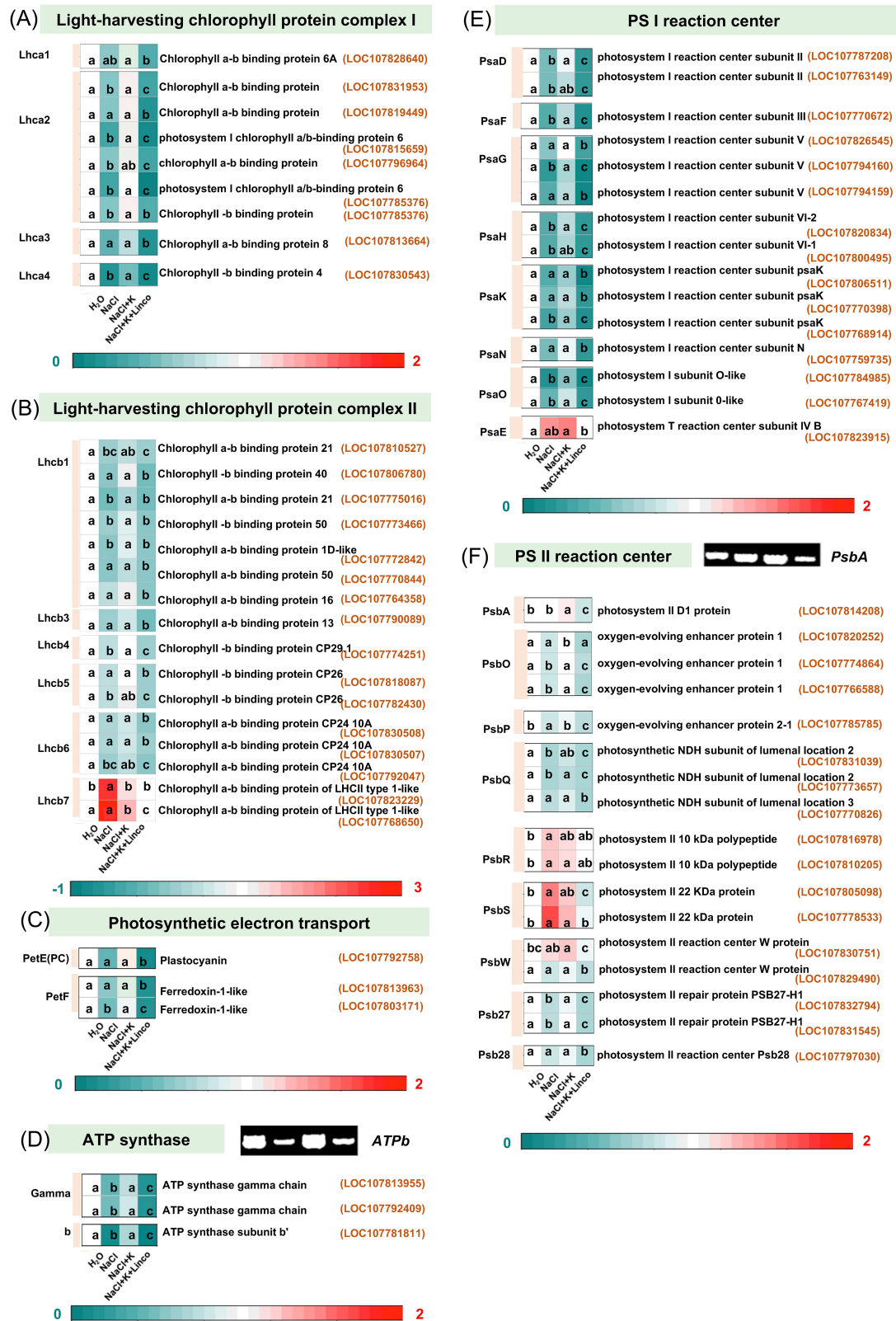


FIGURE 6 Heat map of differential gene expression in tobacco leaves under salt stress. Lhca, light-harvesting chlorophyll protein complex I; Pet, photosynthetic electron transport. The values shown in the heat map become progressively larger from blue to red, and the columns of the heat map correspond to the H₂O, NaCl, NaCl + K, and NaCl + K + Linco treatments, respectively from left to right. Significant differences according to least significant difference (LSD) tests are indicated by different lowercase letters ($p < 0.05$).

Salt stress significantly decreased the overall photochemical yield of PSII in the light-adapted state (Y_{II}); after adding potassium, Y_{II} was significantly higher than that under the NaCl treatment ($p < 0.01$). Lincomycin treatment made Y_{II} lower than that under the NaCl + K treatment but slightly higher than that under the NaCl treatment ($p > 0.05$). The Y_{NPQ} value under the NaCl + K treatment was higher than that under the NaCl treatment, but after the addition of lincomycin, Y_{NPQ} was significantly lower than that of the NaCl + K treatment ($p < 0.01$). The Y_{NO+NF} value in the NaCl treatment was significantly higher than that of the H₂O treatment, but Y_{NO+NF} under treatment with NaCl + K was significantly lower than that under the NaCl treatment, being close to that of the H₂O treatment. The addition of lincomycin made the level of Y_{NO+NF} similar to that under salt stress but significantly higher than those in the H₂O and NaCl + K treatments. Relative to the H₂O treatment, the photochemical efficiency of open PSII traps in the light-adapted state (F_v'/F_m') was significantly lower under salt stress and returned to the level of the H₂O treatment after adding potassium, though not significantly higher than that of the NaCl treatment ($p > 0.05$). In the lincomycin treatment, F_v'/F_m' was significantly lower than that of the NaCl + K treatment ($p < 0.01$). Compared with the H₂O treatment, qP decreased significantly under salt stress; qP in the treatments with potassium was the same as that of the H₂O treatment but higher than that of the NaCl treatment (Figure 5G). Since $Y_{II} = qP \times F_v'/F_m'$, the large decrease in Y_{II} in the NaCl treatment relative to that in the H₂O treatment was mainly due to the substantial decrease in qP .

The MR820 signal can reflect the activity of the photosystem I (PSI) reaction center. Figure 5H,I shows that the difference between the lowest and highest points in the NaCl + K treatment is larger than that in the NaCl treatment, with the NaCl + K + Linco treatment showing the smallest difference.

3.5 | Quantitative analysis of differentially expressed genes

The antenna genes of both photosystems decreased under salt stress, *Lhca2*, *Lhca4*, *Lhcb1* (LOC107775016, LOC107773466, LOC107772842), *Lhcb4*, *Lhcb5* (LOC107782430), and *Lhcb6* (LOC107792047) decreasing significantly (Figure 6A, B). After adding potassium in salt stress conditions, transcription levels of antenna genes of the two photosystems were upregulated as a whole compared with the NaCl treatment, with nine genes significantly upregulated. Compared with the NaCl treatment, 17 antenna genes were significantly decreased under the NaCl + K + Linco treatment, and the expression levels of 24 genes were significantly lower than those under the NaCl + K treatment.

Under NaCl treatment, expression of *PetF* (LOC107803171) was significantly decreased compared with the H₂O treatment, while it was significantly upregulated under the NaCl + K treatment compared with the NaCl treatment (Figure 6C). Additionally, *PetE* and *PetF* expression levels under the NaCl + K + Linco treatment were significantly lower than those under the NaCl and NaCl + K treatments.

Expression of ATP synthase genes was significantly downregulated under the NaCl treatment compared with the H₂O treatment but significantly upregulated compared with salt stress after adding potassium. After inhibition of PSII repair by lincomycin, despite the presence of K⁺ ions, ATP synthase gene expression decreased significantly compared with other treatments (Figure 6D).

Under the NaCl treatment, the PSI reaction center genes *PsaD*, *PsaF*, *PsaG* (LOC107794160), *PsaH*, *PsaK* (LOC107768914), and *PsaO* were significantly downregulated compared with the H₂O treatment but after NaCl + K treatment, seven genes were significantly upregulated compared with the NaCl treatment (Figure 6E). After inhibition of PSII repair by lincomycin, despite the presence of K⁺ ions, the expression of 14 PSI reaction center genes was significantly lower than that under NaCl treatment, and 15 genes were significantly downregulated relative to the NaCl + K treatment.

Under salt stress, eight genes (*PsbO* [LOC107820252, LOC107774864, LOC107766588], *PsbP* [LOC107785785], *PsbQ* [LOC107831039, LOC107773657], *Psb27* [LOC107832794, LOC107831545]) related to the PSII reaction center were significantly downregulated and four genes (*PsbR* [LOC107816978, LOC107810205], *PsbS* [LOC107805098, LOC107778533]) were significantly upregulated compared with the H₂O treatment (Figure 6F). Under NaCl + K, eight genes were significantly upregulated compared with salt stress. By contrast, the expression of 14 genes after the NaCl + K + Linco treatment was significantly lower relative to the NaCl treatment, indicating that potassium plays an important role in the repair of the PSII reaction center.

4 | DISCUSSION

4.1 | A hypothesis on how salt stress exerts its primary effect on photosynthetic processes

Previous work with mulberry leaves (Che, Fan, et al., 2022) led us to propose a hypothesis in which salt stress induces a decrease in the stromal concentration of K⁺ (also observed in the present study on tobacco chloroplasts, Figure 2B) so that insufficient K⁺ rapidly enters the thylakoid lumen via the Two Pore K⁺ channel (TPK3) in rapid exchange for H⁺ exiting the lumen via the ATP synthase. At the same time, since protons are deposited in the lumen and relayed to the lumenal side of the ATP synthase in a stochastic manner (Che, Fan, et al., 2022), the electric potential (the so-called proton diffusion potential) of the lumen becomes more negative, if only momentarily. Consequently, both the sluggish counterion charge compensation in salt-stress conditions and the stochastic replenishment of protons in the lumen retard proton efflux from the lumen. In this hypothesis, the rate of ATP synthesis, driven by a proton circuit around the stroma and lumen (Che, Fan, et al., 2022), is limited by the efflux of protons from the lumen in salt-stress conditions, causing a slow-down of carbon assimilation and, in turn, an accumulation of electrons in the photosynthetic electron transport chain. A highly reduced electron transport chain leads to a

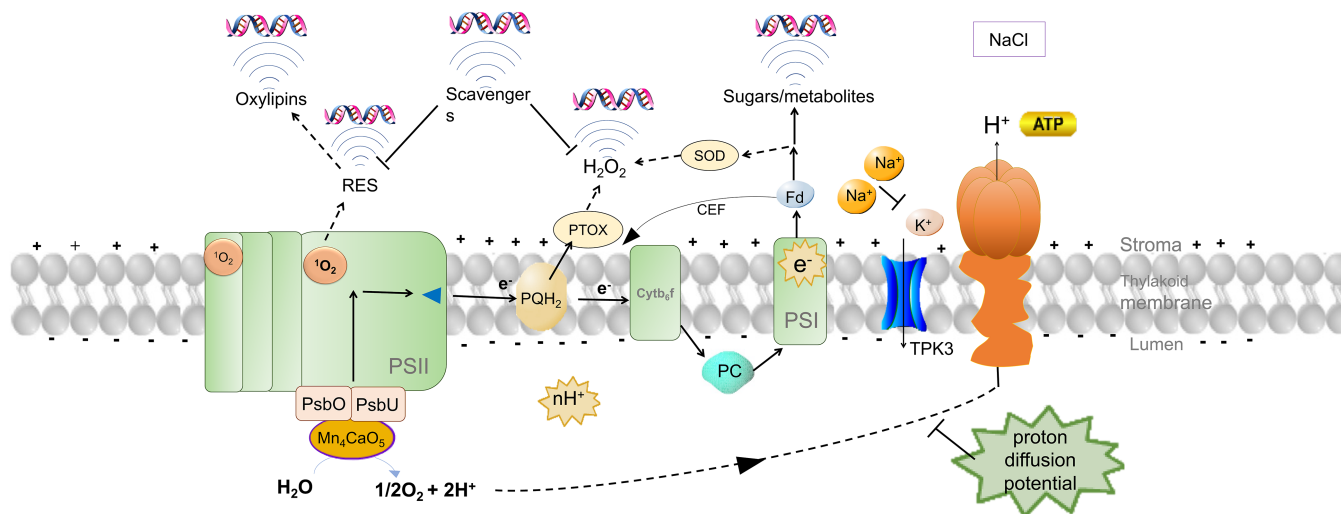


FIGURE 7 A scheme depicting the effects of NaCl treatment on proton translocation, electron transport and retrograde signaling that affects gene expression. Salt stress lowers the stromal $[K^+]$, impairing the influx of K^+ into the lumen via the Two Pore K^+ channel (TPK3) in exchange for H^+ exiting the lumen via the ATP synthase. The impaired charge compensation results in a proton diffusion potential (negative in the lumen) that retards the proton efflux (part of a proton circuit around the stroma and lumen, not shown in this figure, but see Che, Fan, et al., 2022), slowing ATP synthesis. Consequently, carbon assimilation is slowed, so that the electron transport chain is in a highly reduced state during illumination. In such conditions, superoxide is formed on the acceptor side of PSI and/or at the plastid terminal oxidase (PTOX) and converted to H_2O_2 by superoxide dismutase (SOD). In a highly reduced state of the electron transport chain, there is resistance to the downhill flow of electrons on the acceptor side of PSII (indicated by the blue triangle), resulting in more frequent charge recombination (possibly facilitated by misses of the oxygen evolving complex, Mattila et al., 2022) that may result in the formation of highly reactive singlet oxygen 1O_2 . 1O_2 can also be formed in the light-harvesting antenna by triplet chlorophyll after inter-system crossing. Singlet oxygen gives rise to reactive electrophile species (RES), and further products, oxylipins. Scavenging systems can modulate the accumulation of H_2O_2 and RES. All these redox species/systems can serve in retrograde signaling, as can the levels of sugars/metabolites. Re-drawn according to the scheme proposed by Gollan et al. (2015).

deceleration of both linear and cyclic electron transport. For example, a highly reduced plastoquinone (PQ) pool suppresses electron transport by reduction-induced suppression of electron transport (RISE) (Shaku et al., 2016), which is a form of photosynthetic control (Shimakawa & Miyake, 2018), in addition to that form in which a high concentration of protons in the thylakoid lumen retards the oxidation of PQH_2 (West & Wiskich, 1968).

Given the slower efflux of protons from the lumen expected in the present hypothesis in the NaCl treatment, one may expect the pH gradient across the thylakoid membrane to have increased, resulting in increased energy-dependent, nonphotochemical quenching of excitation energy in PSII. However, Y_{NPQ} , the fraction of excitation energy in PSII dissipated in an energy-dependent, regulatory manner, was not increased (Figure 5G). Instead, a highly reduced PQ pool was probably responsible for slower electron linear and cyclic electron transport, tending to decrease the trans-thylakoid pH gradient, such that Y_{NPQ} was, if anything, slightly decreased (Figure 5G). Consistent with a highly reduced PQ pool, the primary quinone acceptor in PSII was in a more reduced state in the NaCl treatment, as indicated by the much lower qP (Figure 5G). A highly reduced photosynthetic electron transport chain, in turn, leads to various changes in photosynthetic function that are observed in salt stress conditions. However, addition of potassium increases the stromal potassium concentration in mulberry chloroplasts and alleviates the salinity-induced proton diffusion

potential difference, thereby preventing many of the salinity-induced effects on chloroplast functional properties (Che, Fan, et al., 2022). In this study on tobacco, we also observed that the K^+ content, though decreased markedly in both leaf tissue and chloroplasts in the NaCl treatment, was increased to the levels of the H_2O treatment when NaCl was supplemented by K^+ (Figure 2B). Below, we further develop this hypothesis based on our observations made in tobacco plants subjected to treatments with H_2O , NaCl, NaCl + K or NaCl + K + lincomycin.

4.2 | Effects of NaCl treatment on the production of ROS and retrograde signaling

A highly reduced electron transport chain leads to the formation of ROS; the resulting oxidative stress can induce damage as well as send retrograde signals to the nucleus to elicit responses at the level of gene expression (Chan et al., 2016; Crawford et al., 2018; Foyer & Shigeoka, 2011; Gollan et al., 2015). In the scheme of Figure 7, for example, superoxide formed after the reduction of molecular oxygen by electrons on the acceptor side of PSI is disproportionated by superoxide dismutase (SOD) to form H_2O_2 . Similarly, electrons from plastoquinol can also reduce oxygen at the plastid terminal oxidase (PTOX) to form superoxide, from

which H_2O_2 is obtained. The upregulation of the genes encoding SOD in tobacco under salt stress was accompanied by an increase in SOD activity (Che, Yao, et al., 2022), facilitating the rapid production of H_2O_2 . At the same time, the downregulation of genes encoding ascorbate peroxidase (APX), glutathione peroxidase and, to a lesser extent, peroxidase was accompanied by a decrease in APX and peroxidase activities (Che, Yao, et al., 2022), thereby slowing the scavenging of H_2O_2 . The combined effect was an increase in the abundance of H_2O_2 by more than twofold (Che, Yao, et al., 2022), which most probably led to the regulation of the expression of other genes and/or the formation of highly reactive hydroxyl free radicals that induce damage. Thus, the smaller MR820 signal under NaCl stress (Figure 5H) could be due to the presence of fewer functional PSI complexes, either through downregulation of PSI genes (Figure 6E) or damage to PSI, or both.

In particular, the backlog of electrons in the electron transport chain in salt stress conditions led to a more reduced state of Q_A in PSII, as indicated by the lower qP (Figure 5G). The “back pressure” against the downhill flow of electrons on the acceptor side of PSII (indicated by the blue triangle in Figure 7) promotes charge recombination to the ground state (directly or via PSII cyclic electron flow) or an excited state of chlorophyll; in either case, energy could be lost in a constitutive, nonregulatory fashion, as indicated by the increase in $Y_{\text{NO}+\text{NF}}$ (Figure 5G) which includes a contribution from any nonfunctional (NF) PSII complexes present. In the case of charge recombination forming an excited state, possibly facilitated by misses of the oxygen-evolving complex (Mattila et al., 2022), there is some chance that triplet chlorophyll (in addition to singlet chlorophyll) is produced; when that occurs, triplet excited chlorophyll may react with triplet oxygen to form highly reactive singlet oxygen, $^1\text{O}_2$ (Figure 7). The $^1\text{O}_2$ so produced might have damaged some PSII complexes, which were then dismantled, thereby decreasing the content of PSII, as was observed in mangrove (Ball et al., 1987) and spinach (Chow et al., 1990) under salinity stress in the presence of very low $[\text{K}^+]$. Nevertheless, it appears that repair of PSII was able to maintain a large proportion of functional PSII (albeit at a lower PSII content) in the NaCl treatment, as evidenced by only a slight decline in F_v/F_m (Figure 5B). Instead, $^1\text{O}_2$ might have led to the production of reactive electrophile species (RES) which served in retrograde signaling (Figure 7). Thus, signaling by RES or the resultant oxylipins could have downregulated the expression of various nuclear-encoded genes in the PSII reaction center (*PsbO*, *PsbP*, *PsbQ*; Figure 6F). *PsbR* is required to maintain the conformation of the PSII complex and to stabilize the binding of both *PsbP* and *PsbQ* (Allahverdiyeva et al., 2007). Previous work has shown that FUD39 mutants obtained by knockout of *PsbP* and *PsbQ* genes still had *PsbR* in the supercomplex, though the total amount of PSII-LHCII decreased significantly (Mayfield et al., 1987); this is consistent with the results of the present study, namely, that the expression of *psbR* gene was increased (Figure 6F). Additionally, H_2O_2 could also have participated in the signaling; indeed, there is cross-talk between

$^1\text{O}_2$ - and H_2O_2 -dependent signaling of stress responses in Arabidopsis (Laloi et al., 2007). In any case, downregulation of gene expression appears to explain the much lower content of PSII per unit leaf area when spinach (Chow et al., 1990) or mangrove (Ball et al., 1987) plants are subjected to salt stress in the presence of a very low potassium concentration in the growth medium. A lower content of PSII tends to deliver fewer electrons to PSI, thereby limiting the production of ROS at the plastid terminal oxidase (PTOX) and on the acceptor side of PSI.

Fewer functional PSII complexes per unit leaf area is insufficient for photoprotection. Rather, limiting light-harvesting capacity obviously diminishes excitation of the photosystems, resulting in less photodamage. Indeed, the chlorophyll content, particularly that of Chl *b*, was decreased in the NaCl treatment (Figure 3). The decrease was almost certainly induced by the downregulation of 21 chlorophyll synthesis genes (Figure 3D), accompanied by the upregulation of genes related to Chl *b* degradation (Figure 3E). Light harvesting is one of the early steps in the synthesis of a photosystem, so the light-harvesting antenna must be regulated according to the physiological state and environmental signals of the plant (Wang, Wang, et al., 2021). The upregulation of *Lhcb7* (Figure 6B) under salt stress may reflect a temporary enhancement of the light-harvesting ability of the plant.

Dissipation of harvested light energy is another means of limiting photodamage. Thus, beta-carotene hydrolase (BCH), which enables the synthesis of components of the xanthophyll cycle (zeaxanthin, antheraxanthin, and violaxanthin), was upregulated in the NaCl treatment (Figure 4C), presumably facilitating energy-dependent nonphotochemical quenching of excitation energy. Similarly, the gene encoding the *PsbS* protein that enhances energy-dependent nonphotochemical quenching was also upregulated in the NaCl treatment (Figure 6F). However, although the expression of *PsbS* was upregulated, the expression of two VDE genes was significantly decreased, while that of *ZE* was increased. We have no explanation for changes in the expression of the VDE and *ZE* genes, which appear not to be conducive to increasing photoprotection by zeaxanthin. The above adjustments in light-harvesting via decreasing antenna pigments and in energy dissipation via *PsbS* appear to limit the excitation energy reaching the PSII reaction center, thereby helping to photoprotect PSII itself. In addition, limiting the flow of electrons from PSII downstream limits the production of ROS. Such “damage-control” responses would ameliorate the situation in which diminished ATP synthesis leads to slower carbon assimilation.

In the NaCl treatment, genes encoding electron-transport components such as plastocyanin and ferredoxin (Figure 6C), and those encoding the ATP synthase (Figure 6D) were downregulated. Possibly, the lower electron transport rates in the NaCl treatment did not necessitate the maintenance of an abundance of these protein complexes, hence the lower abundance of their transcripts. Instead, resources could be better deployed to counteract the effects of salt stress. That is, energy is distributed toward defense and metabolism, away from biosynthetic growth and development (Baena-González, 2010).

4.3 | Prevention of the effects of salt stress by supplemental potassium

In relation to the present hypothesis, supplementation with potassium in the NaCl + K treatment increased the stromal $[K^+]$ in tobacco (Figure 2B), as was also observed in mulberry by Che, Fan, et al. (2022), so that at a given content of the potassium channel TPK3 (Carraretto et al., 2013), more K^+ ions are available to rapidly enter the lumen. In this way, the enhanced influx of K^+ ions into the lumen alleviates the proton diffusion potential that is set up when protons exit the lumen through the ATP synthase. As illumination continues, it is conceivable that $[K^+]$ increases in the lumen; in that situation, a K^+ efflux from and an H^+ influx into the lumen could occur via the KEA3 antiporter (Armbruster et al., 2016; Wang et al., 2017) to prevent excessive buildup of potassium in the lumen while also contributing to the proton electrochemical potential gradient for ATP synthesis.

As the influx of K^+ ions into the lumen rapidly compensates for the efflux of protons from the lumen, retardation of the proton efflux from the lumen by the diffusion potential is ameliorated, so that ATP synthesis and carbon assimilation can speed up, resulting in a less reduced state of the electron transport chain. Thus, under steady illumination qP was much greater while Y_{NO+NF} (Y_{NO} tends to increase as Q_A is in a more reduced state) was much smaller in the NaCl + K treatment than in the NaCl treatment (Figure 5G). Additionally, during a light pulse, the pattern of the kinetic rise in the PSII chlorophyll fluorescence yield in the NaCl + K treatment was restored to be similar to that of the H_2O treatment, as was the extent of photo-oxidation of P700 in PSI (Figure 5I).

In the presence of a less reduced state of the electron transport chain in the NaCl + K treatment, the transcript levels of PSII reaction-center proteins were generally greater than those of the NaCl treatment and, in many cases, similar to those of the control (Figure 6F). The same was true of the transcript levels of light-harvesting chlorophyll–protein complex I (Figure 6A), light-harvesting-chlorophyll–protein complex II (Figure 6B), plastocyanin (Figure 6C), PSI reaction center proteins (Figure 6E), ferredoxin (Figure 6C), and ATP synthase proteins (Figure 6D). These changes in transcript levels are in line with the increases in the contents (per unit leaf area of spinach) of chlorophyll, PSII assayed as atrazine-binding sites, ATP synthase, and to some extent PSI, as the $[K^+]$ in the water-culture medium increased in a background of 250 mM NaCl (Chow et al., 1990). Thus, supplemental potassium prevented the effects of salt stress to a large extent.

4.4 | Effects of lincomycin in the NaCl + K treatment

Photoinactivation of PSII damages not only the D1 protein but also some other proteins of PSII (see, e.g., Yi et al., 2022), necessitating repair of PSII by de novo protein synthesis. Lincomycin inhibits the synthesis of chloroplast-encoded proteins (see, e.g., Yi et al., 2022). The addition

of lincomycin in the NaCl + K treatment led to a substantial decrease in F_v/F_m (Figure 5B), suggesting that a substantial proportion of PSII complexes had been photoinactivated when repair of PSII was prevented. The photoinactivation of PSII, however, was not complete. This was probably due to incomplete access of lincomycin to all the chloroplasts in the leaf tissue. Indeed, Norén et al. (1999) still observed about 21% of D1-protein and about 13% of oxygen evolution activity remaining when *Arabidopsis* plants grown (in 100–120 $\mu\text{mol photons m}^{-2} \text{s}^{-1}$) in a nutrient solution were allowed to take up lincomycin solution (2 mM) overnight and the plants were photoinhibited for 24 h at 1000 $\mu\text{mol photons m}^{-2} \text{s}^{-1}$. With (incomplete) PSII photoinactivation in the NaCl + K + Linc treatment, reduction of the primary electron quinone acceptor Q_A appeared to have been partially inhibited since qP remained high (Figure 5G). This observation is consistent with the suggestion of Cleland et al. (1986) that high-light stress leads to inhibition of Q_A photoreduction. At the same time, the K-band (Figure 5F) and L-band (Figure 5E) had obvious positive bands compared with other treatments, indicating that the OEC was seriously damaged and the connectivity or grouping between adjacent PSIIs was weak at the level of the antenna complex (Momchil et al., 2018). In the absence of an independent verification method, however, these changes in the K and L bands should only be taken as indicators of PSII functionality perturbances.

Interestingly, in the NaCl + K + Linc treatment relative to the NaCl + K treatment, the transcript levels of light-harvesting chlorophyll–protein complex I (Figure 6A), light-harvesting-chlorophyll–protein complex II (Figure 6B), PSII reaction center proteins (Figure 6F), plastocyanin (Figure 6C), PSI reaction center proteins (Figure 6E), ferredoxin (Figure 6C) and ATP synthase proteins (Figure 6D) were generally decreased. As linear electron transport was drastically diminished, H_2O_2 -induced retrograde signaling was unlikely. Instead, 1O_2 produced in PSII was most likely the primary agent leading to retrograde signaling that gave rise to widespread downregulation of gene expression (Figure 7).

The linear electron transport rate is directly proportional to Y_{II} , which is, in turn, directly proportional to qP . As qP was much decreased in the NaCl treatment (Figure 5G), delivery of electrons from PSII would have been drastically decreased, tending to keep P700 in PSI more oxidized. However, the P700 photo-oxidation signal (Figure 5H) was decreased by about 55% in the NaCl treatment and about 65% in the NaCl + K + Linc treatment, relative to the H_2O treatment (Figure 5I). The diminution of the P700 photo-oxidation signal is most probably due to a low abundance of PSI complexes (see Fan et al., 2008 for an example), as a result of the downregulation of gene expression in the present study. Indeed, the photo-oxidizable P700 content, assayed spectrophotometrically in isolated thylakoids, was decreased by 50% (on a leaf-area basis) when the $[K^+]$ in the aerated solution for growing spinach plants was decreased from 10 mM to 0.1 mM in a background of 250 mM NaCl (Chow et al., 1990). Therefore, it appears that when linear electron transport was severely impaired in the NaCl + K + Linc treatment, there was widespread downregulation of gene expression, accompanied by upregulation of genes encoding chlorophyll *b*-degradation enzymes.

5 | CONCLUSIONS

In the present study, we found that treatment with NaCl suppressed the vegetative growth of tobacco seedlings, including expansion of cotyledons and growth of roots, while the chlorophyll content of leaves of seedlings already in their vegetative stage was decreased. The application of potassium ions prevented these effects of NaCl treatment to a large extent. The NaCl treatment also had an impact on the functions of PSII and PSI, as well as affecting the expression of genes associated with light-harvesting, electron transport and ATP synthesis, effects that were prevented by potassium supplementation. In the context of our previous hypothesis (Che, Fan, et al., 2022), supplementary potassium seems to exert its primary effect by ameliorating the high proton diffusion potential difference across the thylakoid membrane caused by salt stress, thereby enhancing ATP synthesis, and consequently accelerating carbon assimilation and avoiding a highly reduced state of the electron-transport chain.

AUTHOR CONTRIBUTIONS

Yanhui Che, Dayong Fan and Wah Soon Chow wrote the manuscript; Dayong Fan and Guangyu Sun designed the research and provided fund support; Yanhui Che, Zhiyuan Teng, Tongtong Yao and Zihan Wang performed the experiments; Yanhui Che, Dayong Fan and Huihui Zhang analyzed the resulting data; Tongtong Yao and Hongbo Zhang helped in preparing the figures.

ACKNOWLEDGMENTS

Acknowledgements We are grateful for research support by Fundamental Research Funds for the Central Universities in China (2572018AA24 to ZYT), National Natural Science Foundation of China (31870430 to DYF and 31870373 to GYS), National Key Research and Development Program of China (2016YFA0600802 to DYF), The Third Xinjiang Scientific Expedition Program of China (Grant No. 2021xjkk0601 to DYF), The Fundamental Research Funds for the Central Universities in China and the National Natural Science Foundation of China. Fundamental Research Funds for the Central Universities in China (2572019DA01 to GYS). Open access publishing facilitated by Australian National University, as part of the Wiley - Australian National University agreement via the Council of Australian University Librarians.

CONFLICT OF INTEREST STATEMENT

The authors declare no conflict of interest.

DATA AVAILABILITY STATEMENT

The authors sent the transcriptome data to NCBI with BioProject ID: PRJNA1003252.

ORCID

Yanhui Che  <https://orcid.org/0000-0003-2966-3767>

Dayong Fan  <https://orcid.org/0000-0002-2591-6029>

Zhiyuan Teng  <https://orcid.org/0000-0002-8208-2235>

Tongtong Yao  <https://orcid.org/0009-0001-2135-8998>

Zihan Wang  <https://orcid.org/0000-0001-8876-7000>

Hongbo Zhang  <https://orcid.org/0000-0002-6956-933X>

Guangyu Sun  <https://orcid.org/0000-0001-8363-0929>

Huihui Zhang  <https://orcid.org/0000-0001-9381-2662>

Wah Soon Chow  <https://orcid.org/0000-0003-4828-5546>

REFERENCES

- Abdul Qados, A.M.S. (2011) Effect of salt stress on plant growth and metabolism of bean plant *Vicia faba* (L.). *Journal of the Saudi Society of Agricultural Sciences*, 10(1), 7–15. Available from: <https://doi.org/10.1016/j.jssas.2010.06.002>
- Acosta-Motos, J.R., Ortuño, M.F., Bernal-Vicente, A., Díaz-Vivancos, P., Sanchez-Blanco, M.J. & Hernandez, J.A. (2017) Plant responses to salt stress: adaptive mechanisms. *Agronomy*, 7(1), 1–38. Available from: <https://doi.org/10.3390/agronomy7010018>
- Ahanger, M.A. & Agarwal, R.M. (2017) Salinity stress induced alterations in antioxidant metabolism and nitrogen assimilation in wheat (*Triticum aestivum* L.) as influenced by potassium supplementation. *Plant Physiology and Biochemistry*, 115, 449–460. Available from: <https://doi.org/10.1016/j.plaphy.2017.04.017>
- Allahverdiyeva, Y., Mamedov, F., Suorsa, M., Styring, S., Vass, I. & Aro, E.-M. (2007) Insights into the function of PsbR protein in *Arabidopsis thaliana*. *Biochimica et Biophysica Acta*, 1767(6), 677–685. Available from: <https://doi.org/10.1016/j.bbabi.2007.01.011>
- Arif, Y., Singh, P., Siddiqui, H., Bajguz, A. & Hayat, S. (2020) Salinity induced physiological and biochemical changes in plants: an omic approach towards salt stress tolerance. *Plant Physiology and Biochemistry*, 156(August), 64–77. Available from: <https://doi.org/10.1016/j.plaphy.2020.08.042>
- Armbruster, U., Leonelli, L., Galvis, V.C., Strand, D., Quinn, E.H., Jonikas, M.C. et al. (2016) Regulation and levels of the thylakoid K⁺/H⁺ antiporter KEA3 shape the dynamic response of photosynthesis in fluctuating light. *Plant & Cell Physiology*, 57(7), 1557–1567. Available from: <https://doi.org/10.1093/pcp/pcw085>
- Baena-González, E. (2010) Energy signaling in the regulation of gene expression during stress. *Molecular Plant*, 3(2), 300–313. Available from: <https://doi.org/10.1093/mp/ssp113>
- Ball, M.C., Chow, W.S. & Anderson, J.M. (1987) Salinity-induced potassium deficiency causes loss of functional Photosystem II in leaves of the grey mangrove, *Avicennia marina*, through depletion of the atrazine-binding polypeptide. *Australian Journal of Plant Physiology*, 14, 351–361. Available from: <https://doi.org/10.1071/pp9870351>
- Bezerra, A.C.M., DaC, V., Junqueira, N.E.G., Hüther, C.M., Borella, J., de Pinho, C.F. et al. (2021) Potassium supply promotes the mitigation of NaCl-induced effects on leaf photochemistry, metabolism and morphology of *Setaria viridis*. *Plant Physiology and Biochemistry*, 160, 193–210. Available from: <https://doi.org/10.1016/j.plaphy.2021.01.021>
- Bistgani, Z.E., Hashemi, M., DaCosta, M., Craker, L., Maggi, F. & Morshedloo, M.R. (2019) Effect of salinity stress on the physiological characteristics, phenolic compounds and antioxidant activity of *Thymus vulgaris* L. and *Thymus daenensis* Celak. *Industrial Crops and Products*, 135(April), 311–320. Available from: <https://doi.org/10.1016/j.indcrop.2019.04.055>
- Carraretto, L., Formentin, E., Teardo, E., Checchetto, V., Tomizioli, M., Morosinotto, T. et al. (2013) A thylakoid-located two-pore K⁺ channel controls photosynthetic light utilization in plants. *Science*, 342, 114–118. Available from: <https://doi.org/10.1126/science.1242113>
- Chan, K.X., Phua, S.Y., Crisp, P., McQuinn, R. & Pogson, B.J. (2016) Learning the languages of the chloroplast: retrograde signaling and beyond. *Annual Review of Plant Biology*, 67, 25–53 Available from: <https://www.annualreviews.org/doi/10.1146/annurev-arplant-043015-111854>

- Che, Y., Fan, D., Wang, Z., Xu, N., Zhang, H., Sun, G. et al. (2022) Potassium mitigates salt stress impacts on photosynthesis by alleviation of the proton diffusion potential in thylakoids. *Environmental and Experimental Botany*, 194, 104708. Available from: <https://doi.org/10.1016/j.envexpbot.2021.104708>
- Che, Y., Wang, H., Zhang, B., Gao, S., Wang, Z., Wang, Y. et al. (2020) Elevated air temperature damage to photosynthetic apparatus alleviated by enhanced cyclic electron flow around photosystem I in tobacco leaves. *Ecotoxicology and Environmental Safety*, 204(4), 111136. Available from: <https://doi.org/10.1016/j.ecoenv.2020.111136>
- Che, Y., Yao, T., Wang, H., Wang, Z., Zhang, H., Sun, G. et al. (2022) Potassium ion regulates hormone, Ca^{2+} and H_2O_2 signal transduction and antioxidant activities to improve salt stress resistance in tobacco. *Plant Physiology and Biochemistry*, 186, 40–51. Available from: <https://doi.org/10.1016/j.plaphy.2022.06.027>
- Chow, W.S., Ball, M.C. & Anderson, J.M. (1990) Growth and photosynthetic responses of spinach to salinity: implications of K^+ nutrition for salt tolerance. *Australian Journal of Plant Physiology*, 17, 563–578. Available from: <https://doi.org/cabdirect/abstract/19910300789>
- Cleland, R.E., Melis, A. & Neale, P.J. (1986) Mechanism of photoinhibition: photochemical reaction center inactivation in system II of chloroplasts. *Photosynthesis Research*, 9, 79–88.
- Crawford, T., Lehotai, N. & Strand, Å. (2018) The role of retrograde signals during plant stress responses. *Journal of Experimental Botany*, 69(11), 2783–2795. Available from: <https://doi.org/10.1093/jxb/erx481>
- Demidchik, V. (2018) ROS-activated ion channels in plants: biophysical characteristics, physiological functions and molecular nature. *International Journal of Molecular Sciences*, 19(4), 17–21. Available from: <https://doi.org/10.3390/ijms19041263>
- Dong, X.X., Jin, H.L. & Wang, H.B. (2016) Research progress on adaptive mechanisms of photosystem to highlight in plants. *Zhiwu Shengli Xuebao/Plant Physiology Journal*, 52(11), 1725–1732. Available from: <https://doi.org/10.13592/j.cnki.pj.2016.1014>
- Fan, D.Y., Hope, A.B., Jia, H. & Chow, W.S. (2008) Separation of light-induced linear, cyclic and stroma-sourced electron fluxes to $P700^+$ in cucumber leaf discs after pre-illumination at a chilling temperature. *Plant & Cell Physiology*, 49(6), 901–911. Available from: <https://doi.org/10.1093/pcp/pcn064>
- Feng, E., Yue, Y., Yang, G. & Xu, Y. (2022) Correlation between SPAD value and chlorophyll content in kiwi leaves. *HortResearch*, 39(12), 22–26.
- Foyer, C.H. & Shigeoka, S. (2011) Understanding oxidative stress and antioxidant functions to enhance photosynthesis. *Plant Physiology*, 155, 93–100. Available from: <https://doi.org/10.1104/pp.110.166181>
- Gollan, P.J., Tikkanen, M. & Aro, E.-M. (2015) Photosynthetic light reactions: integral to chloroplast retrograde signalling. *Current Opinion in Plant Biology*, 27, 180–191. Available from: <https://doi.org/10.1016/j.pbi.2015.07.006>
- Hanin, M., Ebel, C., Ngom, M., Laplaze, L. & Masmoudi, K. (2016) New insights on plant salt tolerance mechanisms and their potential use for breeding. *Frontiers in Plant Science*, 7(11), 1–17. Available from: <https://doi.org/10.3389/fpls.2016.01787>
- Khan, M.I.R., Asgher, M. & Khan, N.A. (2014) Alleviation of salt-induced photosynthesis and growth inhibition by salicylic acid involves glycine-betaine and ethylene in mungbean (*Vigna radiata* L.). *Plant Physiology and Biochemistry*, 80, 67–74. Available from: <https://doi.org/10.1016/j.plaphy.2014.03.026>
- Kornyeyev, D. & Hendrickson, L. (2007) Energy partitioning in photosystem II complexes subjected to photoinhibitory treatment. *Functional Plant Biology*, 34, 214–220. Available from: <https://doi.org/10.1071/FP06327>
- Kunz, H.H., Gierth, M., Herdean, A., Satoh-Cruz, M., Kramer, D.M., Spetea, C. et al. (2014) Plastidial transporters KEA1, -2, and -3 are essential for chloroplast osmoregulation, integrity, and pH regulation in Arabidopsis. *Proceedings of the National Academy of Sciences of the United States of America*, 111(20), 7480–7485. Available from: <https://doi.org/10.1073/pnas.1323899111>
- Laloi, C., Stachowiak, M., Pers-Kamczyc, E., Warzych, E., Murgia, I. & Apel, K. (2007) Cross-talk between singlet oxygen- and hydrogen peroxide-dependent signaling of stress responses in *Arabidopsis thaliana*. *Proceedings of the National Academy of Sciences of the United States of America*, 104, 672–677. Available from: <https://doi.org/10.1073/pnas.0609063103>
- Li, S. (2000) *Principles and Techniques of Plant Physiological Biochemical Experiments*. Beijing: Higher Education Press. (in Chinese).
- Liu, L., Lü, J.-Y. & Zhang, W. (2010) Effects of Cr^{6+} treatment on Cr accumulation and physiological characteristics of celery (*Apium Graveolens*). *Journal of Nuclear Agricultural Sciences*, 24(3), 639–644.
- Mattila, H., Mishra, S., Tyystjärvi, T. & Tyystjärvi, E. (2022) Singlet oxygen production by Photosystem II is caused by misses of the oxygen evolving complex. *The New Phytologist*, 237, 113–125. Available from: <https://doi.org/10.1111/nph.18514>
- Mayfield, S.P., Raftoyiannis, M., Frank, G., Zuber, H. & Rochaix, J.D. (1987) Expression of the nuclear gene encoding oxygen-evolving enhancer protein 2 is required for high levels of photosynthetic oxygen evolution in *Chlamydomonas reinhardtii*. *Proceedings of the National Academy of Sciences of the United States of America*, 84, 749–753. Available from: <https://doi.org/10.1073/pnas.84.3.749>
- Miller, G., Suzuki, N., Ciftci-Yilmaz, S. & Mittler, R. (2010) Reactive oxygen species homeostasis and signalling during drought and salinity stresses. *Plant, Cell & Environment*, 33, 453–467. Available from: <https://doi.org/10.1111/j.1365-3040.2009.02041.x>
- Momchil, P., Lyubka, A.V., Jaco, V. & Vasilij, G. (2018) Effects of different metals on photosynthesis: cadmium and zinc affect chlorophyll fluorescence in durum wheat. *International Journal of Molecular Sciences*, 19(3), 787. Available from: <https://doi.org/10.3390/ijms19030787>
- Norén, H., Svensson, P. & Andersson, B. (1999) Auxiliary photosynthetic functions of *Arabidopsis thaliana*—studies *in vitro* and *in vivo*. *Bioscience Reports*, 19(5), 499–509.
- Oukarroum, A., Golstev, V. & Strasser, R.J. (2013) Temperature effects on pea plants probed by simultaneous measurements of the kinetics of prompt fluorescence, delayed fluorescence and modulated 820 nm reflection. *PLoS One*, 8(3), e59433. Available from: <https://doi.org/10.1371/journal.pone.0059433>
- Raheshan, Z., Nasibi, F., Lakehal, A. & Bellini, C. (2018) Unravelling salt stress responses in two pistachio (*Pistacia vera* L.) genotypes. *Acta Physiologiae Plantarum*, 40(9), 1–13. Available from: <https://doi.org/10.1007/s11738-018-2745-1>
- Shaku, K., Shimakawa, G., Hashiguchi, M. & Miyake, C. (2016) Reduction-induced suppression of electron flow (RISE) in the photosynthetic electron transport system of *Synechococcus elongatus* PCC 7942. *Plant & Cell Physiology*, 57, 1443–1453. Available from: <https://doi.org/10.1093/pcp/pcv198>
- Shimakawa, G. & Miyake, C. (2018) Reduction-induced suppression of electron flow (RISE) is relieved by non-ATP-consuming electron flow in *Synechococcus elongatus* PCC 7942. *Frontiers in Microbiology*, 9, 886. Available from: <https://doi.org/10.3389/fmicb.2018.00886>
- Song, S.S., Long, X.H., Liu, L. & Liu, Z.P. (2011) Effects of Na^+/K^+ on ion distribution in various organs and photosynthetic characteristics of *Catharanthus roseus* at the flowering stage under salt stress. *Acta Pedologica Sinica*, 48(4), 883–887.
- Suo, J., Zhao, Q., David, L., Chen, S. & Dai, S. (2017) Salinity response in chloroplasts: insights from gene characterization. *International Journal of Molecular Sciences*, 18(5), 1011. Available from: <https://doi.org/10.3390/ijms18051011>
- Takahashi, S. & Murata, N. (2008) How do environmental stresses accelerate photoinhibition? *Trends in Plant Science*, 13(4), 178–182. Available from: <https://doi.org/10.1016/j.tplants.2008.01.005>
- Wang, A., Ma, C., Ma, H., Qiu, Z. & Wen, X. (2021) Physiological and proteomic responses of Pitaya to PEG-induced drought stress.

- Agriculture*, 11(7), 632. Available from: <https://doi.org/10.3390/agriculture11070632>
- Wang, C., Yamamoto, H., Narumiya, F., Munekage, Y.N., Finazzi, G., Szabo, I. et al. (2017) Fine-tuned regulation of the K⁺/H⁺ antiporter KEA3 is required to optimize photosynthesis during induction. *The Plant Journal*, 89(3), 540–553. Available from: <https://doi.org/10.1111/tpj.13405>
- Wang, H.R., Zhao, X.Y., Zhang, J.M., Lu, C.H. & Feng, F.J. (2022) Arbuscular mycorrhizal fungus regulates cadmium accumulation, migration, transport, and tolerance in *Medicago sativa*. *Journal of Hazardous Materials*, 435, 129077. Available from: <https://doi.org/10.1016/j.jhazmat.2022.129077>
- Wang, Y., Wang, J.C., Guo, D.D., Zhang, H.B., Che, Y.H., Li, Y.Y. et al. (2021) Physiological and comparative transcriptome analysis of leaf response and physiological adaptation to saline alkali stress across pH values in alfalfa (*Medicago sativa*). *Plant Physiology and Biochemistry*, 167, 140–152. Available from: <https://doi.org/10.1016/j.plaphy.2021.07.040>
- West, K.R. & Wiskich, J.T. (1968) Photosynthetic control by isolated pea chloroplasts. *The Biochemical Journal*, 109, 527–532. Available from: <https://doi.org/10.1042/bj1090527>
- Wu, H., Zhang, X., Giraldo, J.P. & Shabala, S. (2018) It is not all about sodium: revealing tissue specificity and signalling roles of potassium in plant responses to salt stress. *Plant and Soil*, 431, 1–17. Available from: <https://doi.org/10.1007/s11104-018-3770-y>
- Yamane, K., Taniguchi, M. & Miyake, H. (2012) Salinity-induced subcellular accumulation of H₂O₂ in leaves of rice. *Protoplasma*, 249, 301–308. Available from: <https://doi.org/10.1007/s00709-011-0280-7>
- Yi, X.-P., Yao, H.-S., Fan, D.-Y., Zhu, X.-G., Losciale, P., Zhang, Y.-L. et al. (2022) The energy cost of repairing photoinactivated Photosystem II: an experimental determination in cotton leaf discs. *The New Phytologist*, 235(2), 446–456. Available from: <https://doi.org/10.1111/nph.18165>
- Yu, Z.P., Duan, X.B., Luo, L., Dai, S.J., Ding, Z.J. & Xia, G.M. (2020) How plant hormones mediate salt stress responses. *Trends in Plant Science*, 25(11), 1117–1130. Available from: <https://doi.org/10.1016/j.tplants.2020.06.008>
- Zhang, H.H., Li, X., Guan, Y.P., Li, M.B., Wang, Y., Liu, G.J. et al. (2020) Physiological and proteomic responses of reactive oxygen species and antioxidant machinery in leaves of mulberry (*Morus alba* L.) to NaCl and NaHCO₃ stress. *Ecotoxicology and Environmental Safety*, 193, 110259. Available from: <https://doi.org/10.1016/j.ecoenv.2020.110259>
- Zhang, H.H., Wang, Y., Li, X., He, G.Q., Che, Y.H., Teng, Z.Y. et al. (2020) Chlorophyll synthesis and the photoprotective mechanism in leaves of mulberry (*Morus alba* L.) seedlings under NaCl and NaHCO₃ stress revealed by TMT-based proteomics analyses. *Ecotoxicology and Environmental Safety*, 190, 110164. Available from: <https://doi.org/10.1016/j.ecoenv.2020.110164>
- Zhao, C., Zhang, H., Song, C., Zhu, J.-K. & Shabala, S. (2020) Mechanisms of plant responses and adaptations to soil salinity. *The Innovation*, 1, 100017. Available from: <https://doi.org/10.1016/j.plaphy.2021.01.021>
- Zheng, B., Cheng, X., Jiang, D. & Weng, X. (2002) Effects of potassium on Rubisco, RCA and photosynthetic rate of plant. *Journal of Zhejiang Forestry College*, 19(1), 104–108.

How to cite this article: Che, Y., Fan, D., Teng, Z., Yao, T., Wang, Z., Zhang, H. et al. (2023) Potassium alleviates over-reduction of the photosynthetic electron transport chain and helps to maintain photosynthetic function under salt-stress. *Physiologia Plantarum*, 175(4), e13981. Available from: <https://doi.org/10.1111/ppl.13981>